Extreme Mechanics Letters 46 (2021) 101325

Contents lists available at ScienceDirect

Extreme Mechanics Letters

journal homepage: www.elsevier.com/locate/eml

Peel of elastomers of various thicknesses and widths

Tenghao Yin [a,b], Guogao Zhang [a,c], Shaoxing Qu [b], Zhigang Suo [a,*]

[a] John A. Paulson School of Engineering and Applied Sciences, Kavli Institute for Bionano Science and Technology, Harvard University, MA, 02138, USA

[b] State Key Laboratory of Fluid Power & Mechatronic System, Key Laboratory of Soft Machines and Smart Devices of Zhejiang Province, Center for X-Mechanics, and Department of Engineering Mechanics, Zhejiang University, Hangzhou 310027, China

[c] State Key Laboratory of Chemical Engineering, College of Chemical and Biological Engineering, Zhejiang University, Hangzhou 310027, China

ARTICLE INFO

Article history:
Received 27 January 2021
Received in revised form 14 April 2021
Accepted 17 April 2021
Available online 21 April 2021

Keywords:
Soft materials
Width- and thickness-dependent toughness
Stress state
Damage

ABSTRACT

We peel a highly stretchable silicone (Ecoflex), thickness H and width B, sandwiched between two inextensible films. When the peel front advances steadily in the elastomer, the peel force reaches a plateau F_{ss}, and the ratio $2F_{ss}/B$ is commonly reported as the toughness of the elastomer. Our data show that this "peel toughness" is not always a material constant, but can depend on the thickness H and width B. We interpret the data in terms of two fundamental ideas in fracture mechanics. First, as the ratio B/H increases, the deformation in the elastomer changes from the plane stress to the plane strain conditions, so that the stress state ahead the peel front changes from biaxial to triaxial tension. We show that the elastomer under triaxial tension reaches higher stress and damages more than the elastomer under biaxial tension. Second, when the inelastic zone around a peel front is not much smaller than H, peel is under large-scale inelasticity conditions, and the material ahead the peel front deforms in nearly a homogeneous state. We show our data measured using various thicknesses collapse into a single curve on the plane with axes Γ/H and B/H.

1. Introduction

Stretchable materials, such as gels and elastomers, are often used as thin layers. Examples include adhesives [1,2], coatings [3,4], ionotronics [5–8], robots [9,10], cell culture scaffolds [11], and displays [12]. A convenient test is to peel a material sandwiched between two inextensible films [13–16]. Here we peel a highly stretchable silicone (Ecoflex), thickness H and width B, sandwiched between two plastic films (Section 2). When the peel front advances steadily in the elastomer, the peel force reaches a plateau F_{ss}, and the ratio $2F_{ss}/B$ is commonly reported as the toughness of the elastomer (Fig. 1). Our data show that this "peel toughness" is not always a material constant, but can depend on H and B (Section 3). When the ratio B/H increases, the deformation in the elastomer changes from the plane stress to the plane strain conditions, so that the stress state ahead the peel front changes from biaxial to triaxial tension. The two types of stress state cause different degrees of damage, as corroborated by the markedly different load–unload curves of a thin film and a disk-shaped sample. When the inelastic zone around a peel front is not much smaller than H, peel is under the large-scale inelasticity conditions, and our data measured using various thicknesses collapse to a single curve on the plane with axes Γ/H and B/H.

2. Materials and experimental methods

We choose silicone rubber (Ecoflex™ 00–20, Smooth On) as a model material. The precursor comes as two liquids, A and B. We mix them by 1:1 weight ratio using a mixer (ARE-250; Thinky) at 2000 r/min for 1 min, and degas the mixture at 2000 r/min for another 1 min. The mixture is further degassed for 8 min in a desiccator driven by a vacuum pump. We pour the mixture into a rectangular acrylic mold, cure the mixture in an oven at 65 °C for 4 h, and take the elastomer out of the mold.

We first conduct pure shear tests on a thin silicone film. The deformable part of the sample has a dimension of width 100 mm × height 20 mm × thickness 1 mm in the reference state and is loaded along the height direction. We obtain the initial shear modulus, $\mu = 9.11$ kPa, of the silicone elastomers.

Following Rivlin and Thomas [17], we conduct 180-degree peel. To introduce a cut, we insert a thin paraffin film (Bemis, Parafilm M) into the mixture before cure and remove the paraffin film after cure. In the undeformed state, a layer of an elastomer, length L, thickness H, width B, has a precut of length $C = 20$ mm (Fig. 1a). We spray adhesion promoter (7701™, Loctite) on the sample surfaces, wait for the evaporation of promoter solvent, and glue the backing layers on sample surfaces using an adhesive (406™, Henkel Loctite). The backing layer is flexible but inextensible film (3M AF 4300 Write-on transparency films and Dupont Kapton Film). The sample is peeled by a tensile machine

* Corresponding author.
E-mail address: suo@seas.harvard.edu (Z. Suo).

https://doi.org/10.1016/j.eml.2021.101325
2352-4316/

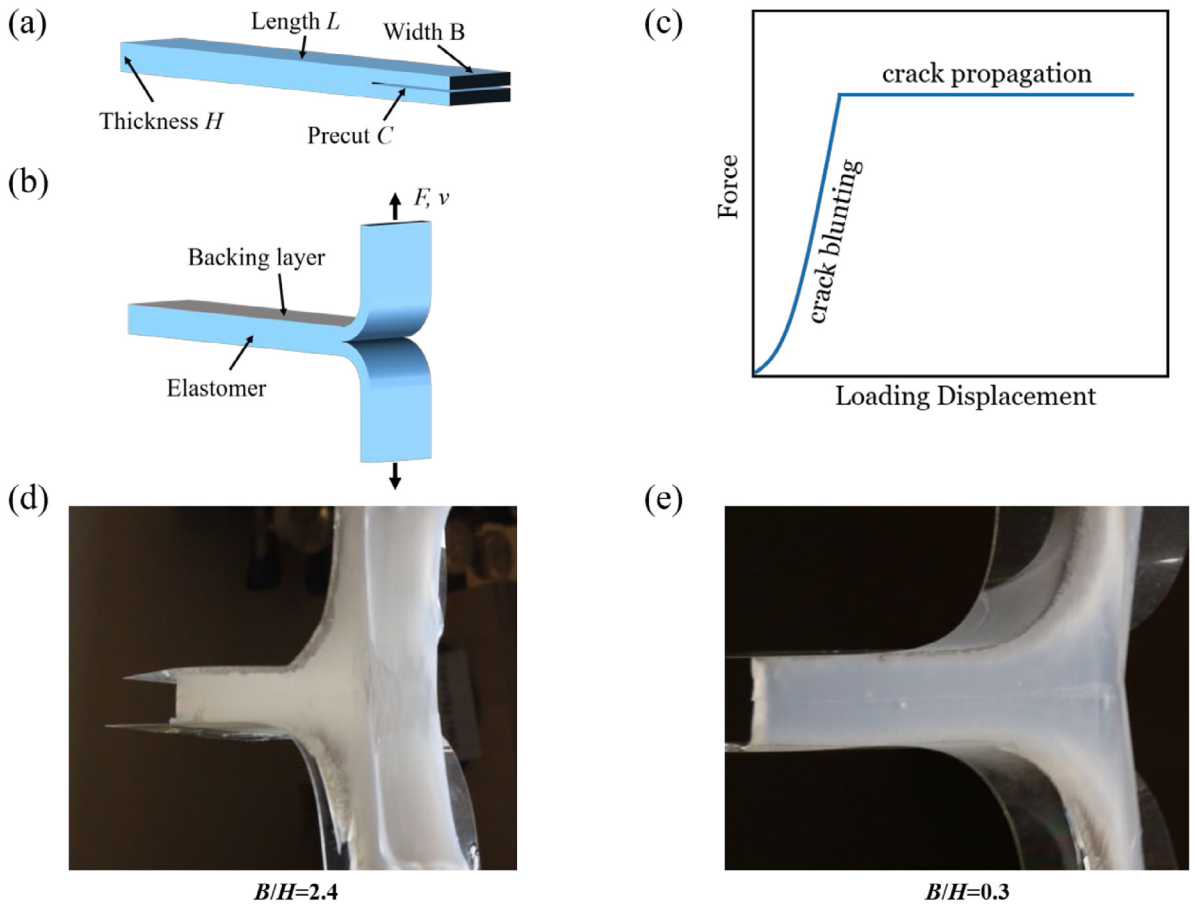

Fig. 1. 180-degree peel. (a) In the undeformed state, a layer of an elastomer has length L, thickness H, and width B. A precut crack of length C is introduced in the elastomer by inserting a low-adhesion film when the elastomer is cured. (b) In the deformed state, the elastomer is sandwiched between two plastic layers. As a machine pulls the plastic layers at a constant velocity v, the force F is recorded. (c) A schematic force–displacement curve. When the cut blunts but does not advance, the force increases with the displacement. When the peel front advances in a steady state, the force reaches a plateau as the displacement increases. (d) A wide sample ($B = 15.24$ mm) deforms under the plane strain conditions, so that the elastomer ahead the peel front is under triaxial tension. (e) A narrow sample ($B = 1.91$ mm) deforms under the plane stress conditions, so that the elastomer ahead the peel front is under biaxial tension. The thickness of the elastomer is $H = 6.35$ mm in (d) and (e).

(Instron 5966) at velocity v, with the rate of peel set at $H/v = 0.3$ s (Fig. 1b). During peel, the two arms are aligned vertically and the load cell records the peel force F. The peel force is plotted as a function of the loading displacement (Fig. 1c). When the cut blunts but does not advance, the force increases with the displacement. When the peel front advances in a steady state, the force reaches a plateau as the displacement increases. When B/H is large, the elastomer peels approximately under the plane strain conditions (Fig. 1d). When B/H is small, the elastomer peels approximately under the plane stress conditions (Fig. 1e).

3. Peel toughness varies with width and thickness

Fig. 2 shows the force–displacement curves for samples of fixed thickness $H = 6.35$ mm and various widths B. For each width, three samples are tested. For samples of small widths, when the peel front advances, the force goes up and down substantially. This change in the peel force corresponds to up–down jumps of the peel front (Fig. 3). Even when peel front is close to a backing layer, cohesive failure is observed. A similar phenomenon has been studied in an epoxy sandwiched between two layers of metal [18,19]. The crack path selection in such a brittle adhesive layer is considered to be associated with the applied stress intensity factors and the mismatch of elastic moduli between the adhesive layer and the substrate. Here we will not study this phenomenon. For samples of large widths, the fluctuation of the peel force is small, and the peel advances smoothly.

The energy release rate for the peel test is determined as follows [17]. The energy release rate G is defined by $F\mathrm{d}D = \mathrm{d}U + GB\mathrm{d}C$, where F is the peel force, D is the loading displacement, B is the width of the sample, C is the length of the cut, and U is the elastic energy in the sample. Specifically, this definition of G is applicable when the peel advances in steady state. In the steady state, the elastic energy in the sample is invariant, $\mathrm{d}U = 0$. Because the backing layers are inextensible, the loading displacement is the twice the advance of the peel, $\mathrm{d}D = 2\mathrm{d}C$. Consequently, the energy release rate in steady state peel is given by $G = 2F/B$. In the steady state, the peel force reaches a plateau, F_{ss}, and the energy release rate is called the toughness, $\Gamma = 2F_{ss}/B$.

When the peel front advances, we use the average force to calculate the toughness. The toughness Γ is plotted as a function of the width B (Fig. 4). The toughness increases with the width when B is small, and becomes a constant independent of the width when B is large. The toughness of a sample of large width can be one order of magnitude higher than the toughness of a sample of small width.

The increase of toughness with the width B is interpreted as follows. The elastomer is a three-dimensional network of polymer chains. Consider a material particle ahead the peel front. The stress in the loading direction is nonzero. The deformation in the direction of peel is constrained by the backing layers, so

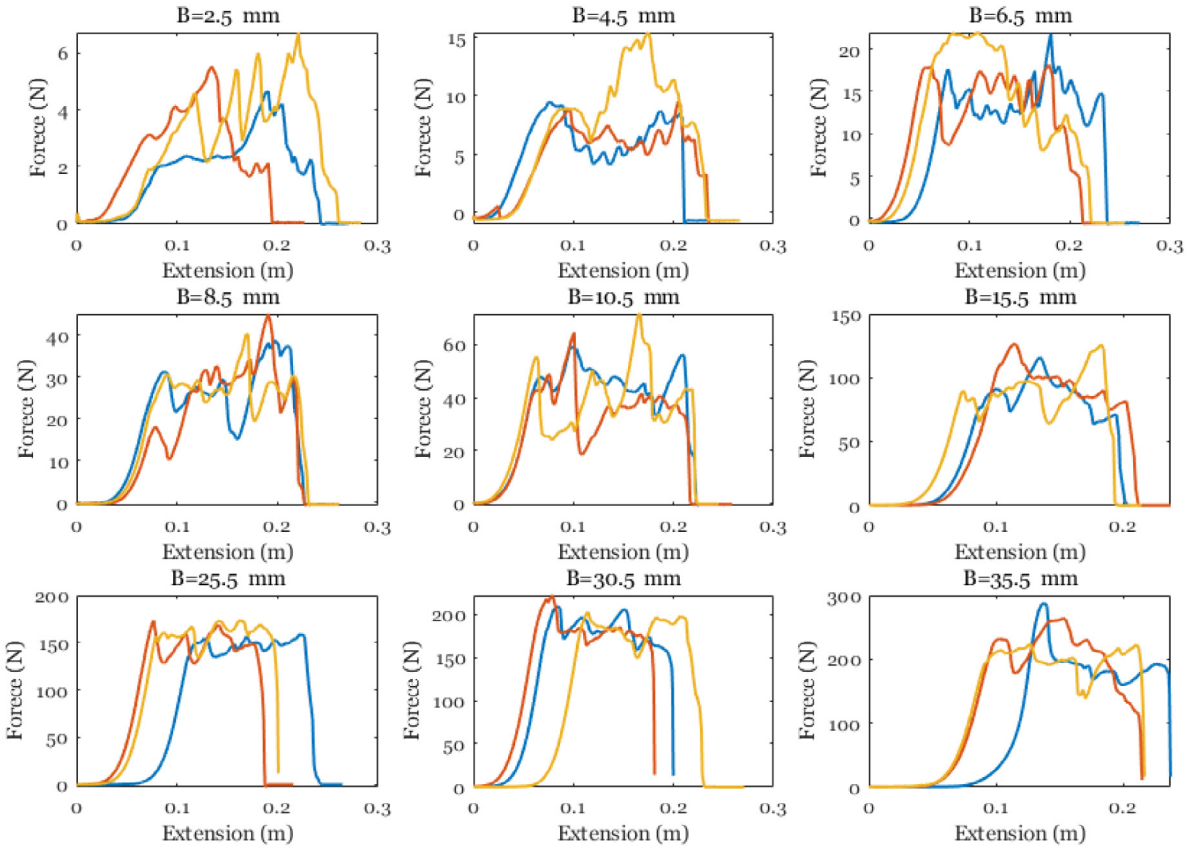

Fig. 2. Force–displacement curves for samples with various widths B, and a fixed thickness $H = 6.35$ mm. For each width, three samples are tested.

that the stress in the direction of peel is also nonzero. When the width B is large, the material particle deforms under the plane strain conditions (Fig. 1d), so that the stress in the width direction is nonzero. When the width B is small, the material particle deforms under the plane stress conditions (Fig. 1e), so that the stress in the width direction is zero. Consequently, material ahead the peel front is under triaxial tension in a wide sample, but is under biaxial tension in a narrow sample. The polymer network can sustain higher stress in triaxial tension than in biaxial tension. It is likely that the former causes more damage than the latter. To corroborate this finding, we load and unload a film with dimensions 20 mm $\times$ 20 mm $\times$ 1.5 mm and a disk-shaped sample with a diameter 40 mm and thickness 3.175 mm. Both samples are stretched to 4 and then unloaded (Fig. 5). The hysteresis of the disk-shaped sample is $\sim$46%, and that of the film is $\sim$22%. The stress in the disk-shaped sample is higher than that in the film. In the disk-shaped sample, we do not observe cavitation. A similar effect is known in metals. When a sheet of metal with a precut crack is pulled in tension, the toughness is a function of the thickness of the sheet. For metals, this effect is called the 'thickness effect of toughness'. A typical toughness–thickness curve for a metal has the following trend. As the thickness increases, the toughness increases, reaches a peak, drops, and reaches a plateau. When the thickness is small, the material ahead the crack tip is in biaxial tension, rupture is caused by necking, and the toughness increases with the thickness [20]. When the thickness further increases, triaxial tension at the crack tip dominates the fracture process. The triaxial tension causes the nucleation [21], growth [22] and coalescence [23] of voids, giving a lower toughness. The thickness-dependent toughness in metals has been analyzed [24–26]. Note that, for an elastomer studied in this paper, the toughness does not reach a peak; rather, the toughness increases with the width of the peel sample, and asymptotes to a plateau as the width increases. At this writing, this difference between the elastomer and a metal is not understood.

We further peel the elastomer with various thicknesses H (Fig. 6). For every thickness H, the toughness–width curve takes a similar form. When $B >> H$, the toughness plateaus, and the plateau increases with the thickness H. This effect has been discussed before [14]. When a sample with a crack is loaded, the stress concentrates around the crack tip. In a region around the crack, the material is inelastic. Outside this region, the material is considered elastic. The sample is said to be under the small-scale inelasticity conditions when all the sample dimensions are much larger than the size of the inelastic region. Under the small-scale inelasticity conditions, the toughness is a material property independent of the sample size. The size of this region scales with Γ/W_f, where Γ is the toughness measured using a sample with a precut crack, and W_f is work of fracture measured using a sample without a precut crack. When both Γ and W_f are material constants, the ratio Γ/W_f is also a material constant, called the fractocohesive length [27,28]. For a tough material, this length is large. For example, Γ/W_f $\sim$10 mm for a tough hydrogel, which is on the same order of that for ductile steels and natural rubbers. For a brittle material, this length is small. For example, Γ/W_f $\sim$1 nm for a silica glass. When one of the sample dimensions is not much larger than the inelastic zone size, the measured toughness does depend on the sample size, and the material is said to be under the large-scale inelasticity conditions. From our previous study, when the thickness H is smaller than the fractocohesive length, $\Gamma = W_f H + \Gamma_0$, where Γ_0 is called the peel threshold [14]. The peel threshold is the toughness with vanishing thickness. We identify Γ_0 as the energy needed to break one layer of chains in the Lake–Thomas model [29].

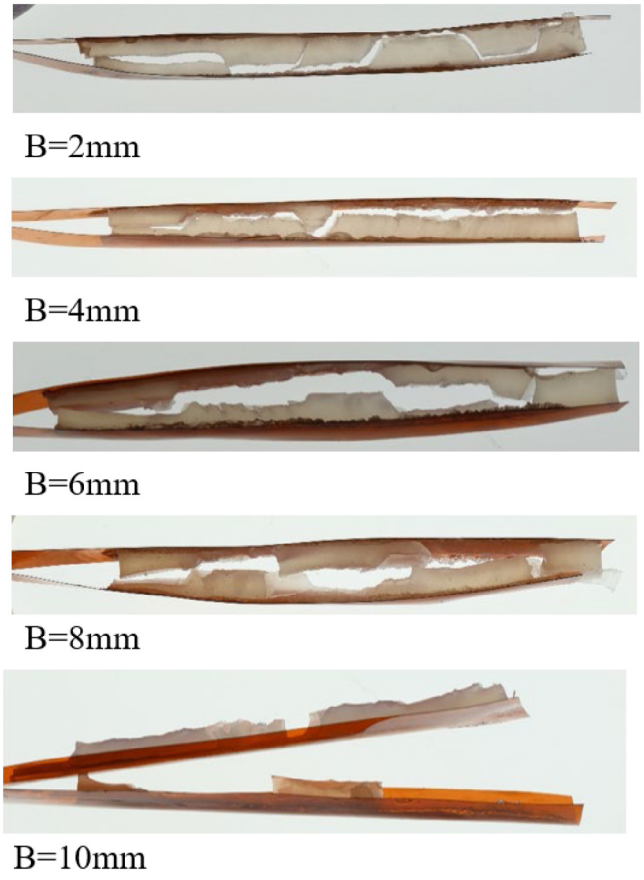

Fig. 3. Photos for samples after peel test. For samples of small widths, the peel front often goes up and down. The thickness is $H = 6.35$ mm.

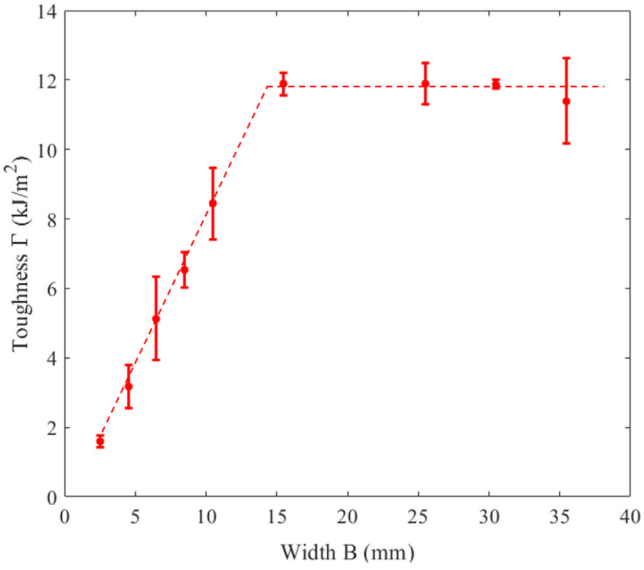

Fig. 4. Toughness varies with the width B. The thickness is $H = 6.35$ mm. The dashed line is drawn to guide the eye.

Under the large-scale inelasticity conditions, the material ahead the peel front is nearly in a homogeneous state. Consequently, the peel test is analogous to a tensile test of a homogeneous sample. In equation $\Gamma = W_f H + \Gamma_0$, we drop the small quantity Γ_0, and write $\Gamma/H = 2F_{ss}/BH = W_f$. We plot Γ/H as a function of B/H for all the curves (Fig. 7). The curves for three thicknesses, $H = 3.675$ mm, 4.675 mm, and 6.35 mm, collapse into one curve. The vertical axis is interpreted as W_f, and the horizontal axis B/H affects the stress state. That is, the work of fracture is affected by the stress state. When $B << H$, the material is under biaxial tension, and the work of fracture is low. When $B >> H$, the material is under triaxial tension, and the work of fracture is high.

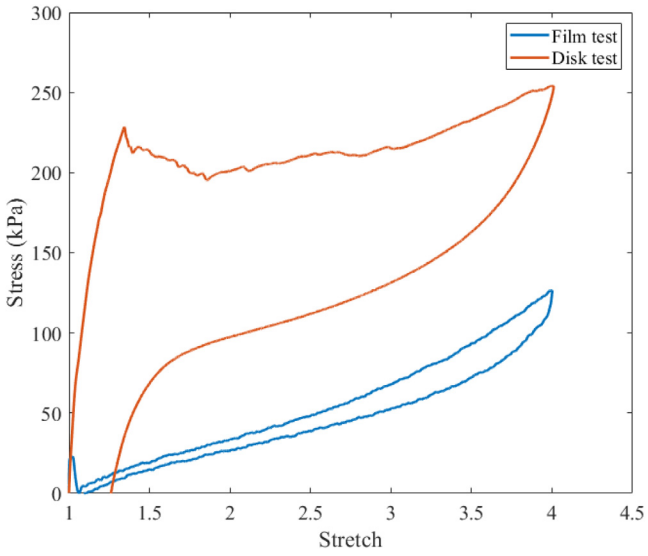

Fig. 5. Load–unload test of a film with dimensions 20 mm × 20 mm × 1.5 mm and a disk-shaped sample of diameter 40 mm and thickness 3.175 mm.

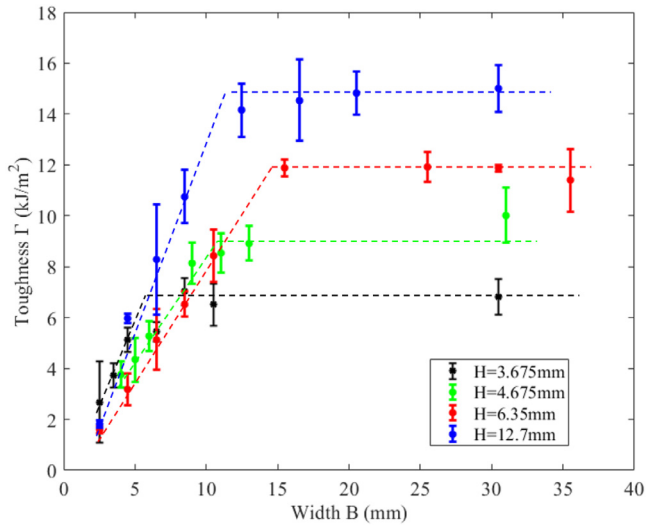

Fig. 6. Toughness varies with the width B. The thickness is $H = 3.675$ mm, 4.675 mm, 6.35 mm, and 12.7 mm. The dashed lines are drawn to guide the eye. (For interpretation of the references to color in this figure legend, the reader is referred to the web version of this article.)

Also note that the curve for $H = 12.7$ mm does not collapse with the other three curves. This exception is interpreted as that samples of $H = 12.7$ mm are under the small-scale inelasticity conditions. For a wide sample, $B >> H$, the elastomer is peeled under the plane strain conditions. The toughness is $\Gamma = 14.64$ kJ/m^2 (plateau of blue curve in Fig. 6), and the work of fracture is $W_f = 1.9$ MJ/m^3 (plateau in Fig. 7), so that the fractocohesive length is $\Gamma/W_f = 7.7$ mm.

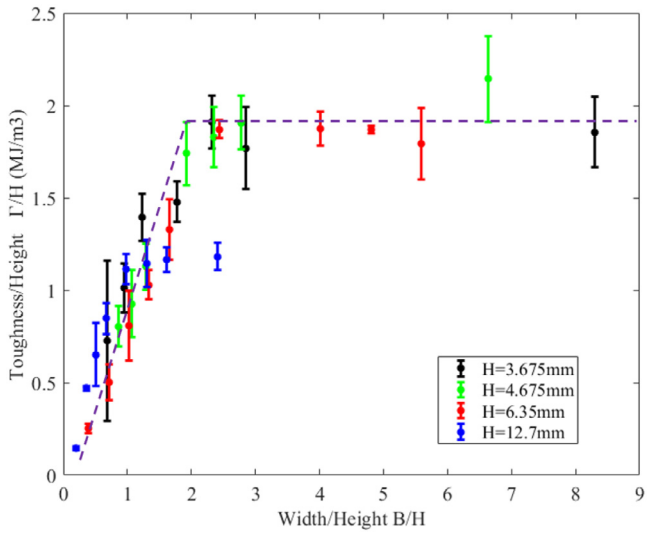

Fig. 7. Γ/H as a function of B/H. In this normalization, the curves for samples under large-scale inelasticity conditions collapse into a single curve.

4. Conclusion

We have peeled a stretchable silicone of various thicknesses H and widths B, and find that the peel toughness varies with both thickness and width. When B/H is large, the material peels under the plane strain conditions, and the stress state is triaxial. When B/H is small, the material peels under the plane stress conditions, and the stress state is biaxial. We show that the elastomer under triaxial tension reaches higher stress and damages more than the elastomer under biaxial tension. Under the large-scale inelasticity conditions, the material ahead the peel front deforms in nearly a homogeneous state, and the toughness–width curves collapse into a single curve in the plane with axes Γ/H and B/H. Our work illustrates effects of geometry on toughness.

Declaration of competing interest

The authors declare that they have no known competing financial interests or personal relationships that could have appeared to influence the work reported in this paper.

Acknowledgments

Work at Harvard was supported by National Science Foundation (NSF) MRSEC (DMR-2011754). T. Yin and S. Qu are supported by the National Natural Science Foundation of China (nos. 11525210 and 91748209), Key Research and Development Program of Zhejiang Province (2020C05010) and the Fundamental Research Funds for the Central Universities (No. 2020XZZX005-02). T. Yin thanks China Scholarship Council for a two-year scholarship as a visiting student at Harvard University.

References

[1] A.N. Gent, G.R. Hamed, Peel mechanics for an elastic–plastic adherend, J. Appl. Polym. Sci. 21 (10) (1977) 2817–2831.
[2] A.N. Gent, G.R. Hamed, Peel mechanics of adhesive joints, Polym. Eng. Sci. 17 (7) (1977) 462–466.
[3] X. Yao, et al., Hydrogel paint, Adv. Mater. 31 (39) (2019) 1903062.
[4] Y. Yu, et al., Multifunctional hydrogel skins on diverse polymers with arbitrary shapes, Adv. Mater. 31 (7) (2019) 1807101.
[5] C. Keplinger, et al., Stretchable, transparent, ionic conductors, Science 341 (6149) (2013) 984–987.
[6] S. Lin, et al., Stretchable hydrogel electronics and devices, Adv. Mater. 28 (22) (2016) 4497–4505.
[7] C. Yang, Z. Suo, Hydrogel ionotronics, Nat. Rev. Mater. 3 (6) (2018) 125.
[8] T. Yin, et al., Ultrastretchable and conductive core/sheath hydrogel fibers with multifunctionality, J. Polym. Sci. B: Polym. Phys. 57 (5) (2019) 272–280.
[9] T. Li, et al., Fast-moving soft electronic fish, Sci. Adv. 3 (4) (2017) e1602045.
[10] M. Wehner, et al., An integrated design and fabrication strategy for entirely soft, autonomous robots, Nature 536 (7617) (2016) 451–455.
[11] X. Zhao, et al., Active scaffolds for on-demand drug and cell delivery, Proc. Natl. Acad. Sci. U S A 108 (1) (2011) 67–72.
[12] T. Yin, et al., Soft display using photonic crystals on dielectric elastomers, ACS Appl. Mater. Interfaces 10 (29) (2018) 24758–24766.
[13] A.N. Gent, G.R. Hamed, Peel mechanics, J. Adhes. 7 (2) (1975) 91–95.
[14] J. Liu, et al., Polyacrylamide hydrogels. II. Elastic dissipater, J. Mech. Phys. Solids 133 (2019) 103737.
[15] Z. Liu, et al., Mechanics of zero degree peel test on a tape—effects of large deformation, material nonlinearity, and finite bond length, Extr. Mech. Lett. 32 (2019) 100518.
[16] B. Chen, et al., Molecular staples for tough and stretchable adhesion in integrated soft materials, Adv. Healthcare Mater. 8 (19) (2019) 1900810.
[17] R. Rivlin, A.G. Thomas, Rupture of rubber. I. Characteristic energy for tearing, J. Polym. Sci. 10 (3) (1953) 291–318.
[18] H. Chai, A note on crack trajectory in an elastic strip bounded by rigid substrates, Int. J. Fract. 32 (3) (1986) 211–213.
[19] N.A. Fleck, J.W. Hutchinson, S. Zhigang, Crack path selection in a brittle adhesive layer, Int. J. Solids Struct. 27 (13) (1991) 1683–1703.
[20] T. Pardoen, Y. Marchal, F. Delannay, Essential work of fracture compared to fracture mechanics—towards a thickness independent plane stress toughness, Eng. Fract. Mech. 69 (5) (2002) 617–631.
[21] S. Goods, L. Brown, Overview no. 1: The nucleation of cavities by plastic deformation, Acta Metall. 27 (1) (1979) 1–15.
[22] J.R. Rice, D.M. Tracey, On the ductile enlargement of voids in triaxial stress fields*, J. Mech. Phys. Solids 17 (3) (1969) 201–217.
[23] G. Le Roy, et al., A model of ductile fracture based on the nucleation and growth of voids, Acta Metall. 29 (8) (1981) 1509–1522.
[24] J.I. Bluhm, A Model for the Effect of Thickness on Fracture Toughness, Watertown Arsenal Labs Mass, 1961.
[25] G. Hahn, et al., Rapid crack propagation in a high strength steel, Metall. Trans. 5 (2) (1974) 475–482.
[26] M. Lai, W. Ferguson, Effect of specimen thickness on fracture toughness, Eng. Fract. Mech. 23 (4) (1986) 649–659.
[27] C. Chen, Z. Wang, Z. Suo, Flaw sensitivity of highly stretchable materials, Extr. Mech. Lett. 10 (2017) 50–57.
[28] C. Yang, T. Yin, Z. Suo, Polyacrylamide hydrogels. I. Network imperfection, J. Mech. Phys. Solids 131 (2019) 43–55.
[29] G. Lake, A. Thomas, The strength of highly elastic materials, Proc. R. Soc. Lond. Ser. A Math. Phys. Eng. Sci. 300 (1460) (1967) 108–119.